Published in final edited form as:
Vis Neurosci. 2009 ; 26(2): 177–187. doi:10.1017/S0952523809090026.

Differential Expression of Three T-Type Calcium Channels in Retinal Bipolar Cells in Rat

Caiping Hu*, **Anding Bi**, and **Zhuo-Hua Pan**
Department of Anatomy and Cell Biology, Wayne State University School of Medicine, Detroit, MI 48201

Abstract

Retinal bipolar cells convey visual information from photoreceptors to retinal third-order neurons, amacrine and ganglion cells, with graded potentials through diversified cell types. To understand the possible role of voltage-dependent T-type Ca^{2+} currents in retinal bipolar cells, we investigated the pharmacological and biophysical properties of T-type Ca^{2+} currents in acutely dissociated retinal cone bipolar cells from rat using whole-cell patch-clamp recordings. We observed a broad group of cone bipolar cells with prominent T-type Ca^{2+} currents (T-rich) and another group with prominent L-type Ca^{2+} currents (L-rich). Based on the pharmacological and biophysical properties of the T-type Ca^{2+} currents, T-rich cone bipolar cells could be divided into three subgroups. Each subgroup appeared to express a single dominant T-type Ca^{2+} channel subunit. The T-type calcium currents could generate low threshold regenerative potentials or spikes. Our results suggest that T-type Ca^{2+} channels may play an active and distinct signaling role in second-order neurons of the visual system, in contrast to the common signaling by L-rich bipolar cells.

Keywords

T-type calcium channels; cone bipolar cells; retina; rodents; patch-clamp

Introduction

Visual information is processed through multiple parallel pathways in the retina (Wässle, 2004). Retinal bipolar cells, which relay visual information from photoreceptors to retinal third-order neurons, consist of multiple types of cells with diverse physiological properties (Wu et al., 2000; Awatramani & Slaughter, 2000; Euler & Masland, 2000). The existence of multiple bipolar cell types is believed to be the important anatomical substrates for segregating visual information into parallel pathways. Increasing evidence suggests that voltage-dependent membrane channels may contribute to the diverse physiological properties of bipolar cells (Burrone & Lagnado, 1997; Mao et al., 1998; Zenisek & Matthews, 1998; Protti et al., 2000; Ma et al., 2005). Among these channels, voltage-dependent Ca^{2+} channels may be particularly important, since the activation of these channels could depolarize the membrane potentials and thereby shape the response waveform of bipolar cells, as well as initiate neurotransmitter release at their axon terminals.

Voltage-dependent Ca^{2+} channels in retinal bipolar cells consist primarily of the sustained L-type (Kaneko et al., 1991; Heidelberger & Matthews, 1992; Tachibana et al., 1993; Protti et

Address correspondence: Zhuo-Hua Pan, Ph.D., Department of Anatomy and Cell Biology, Wayne State University School of Medicine, 540 E. Canfield Avenue, Detroit, MI 48201, Tel. 313-577-9830; Fax 313-577-3125, zhpan@med.wayne.edu.
*Current address: Department Of Physiology and Biophysics, State University of New York at Buffalo, Buffalo, NY 14214.

al., 2000) and the transient T-type (Kaneko et al., 1989; Maguire et al., 1989; Protti & Llano, 1998; Satoh et al., 1998, Pan, 2000). Previous studies have reported the heterogeneous expression of L- and T-type currents among bipolar cells (Protti et al., 1998; Pan, 2000). Three Ca^{2+} channel α subunits, α1G ($Ca_V3.1$), α1H ($Ca_V3.2$), and α1I ($Ca_V3.3$), are known to underlie T-type Ca^{2+} currents (Perez-Reyes et al., 1998; Perez-Reyes, 2003). The Ca^{2+} current of each α subunit exhibits unique pharmacological and biophysical properties (Lee et al., 1999; McRory et al., 2001; Todorovic et al., 2001). The mRNA of all three of these α subunits has been detected in the retina and in retinal bipolar cells (Pan et al., 2001). The cellular expression pattern of L-type versus T-type Ca^{2+} currents among retinal cone bipolar cells, however, remains unclear. Furthermore, the detailed pharmacological and biophysical properties of T-type Ca^{2+} currents in retinal bipolar cells still remain to be studied.

In this study, we used whole-cell patch-clamp recordings to investigate the properties of T-type Ca^{2+} currents in acutely dissociated retinal bipolar cells from rats. We observed one broad group of cone bipolar cells with prominent T-type Ca^{2+} currents (T-rich), in contrast to another broad group of cone bipolar cells with prominent L-type Ca^{2+} currents (L-rich). Furthermore, the T-rich cone bipolar cells could be divided into three subgroups, each of which predominantly expresses a single dominant T-type Ca^{2+} channel subunit.

Materials and Methods

Preparation of isolated bipolar cells

Bipolar cells were isolated from Long Evans rats (>4 weeks old) using previously described dissociation methods (Pan, 2000). All animal experiments and procedures were approved by the Institutional Animal Care Committee at Wayne State University, and were in accordance with the NIH Guide for the Care and Use of Laboratory Animals. In brief, animals were deeply anesthetized with CO_2 and killed by decapitation. Retinas were removed and placed in Hanks' solution (normal Hanks') containing (in mM): 138 NaCl, 1 $NaHCO_3$, 0.3 Na_2HPO_4, 5 KCl, 0.3 KH_2PO_4, 1.25 $CaCl_2$, 0.5 $MgSO_4$, 0.5 $MgCl_2$, 5 HEPES, 22.2 glucose, and 0.001% (v/v) phenol red, with the pH adjusted to 7.2 using 0.3 N NaOH. The retinas were incubated for ~50 min at 34-37 °C in an enzyme solution that consisted of Hanks' solution supplemented with 0.2 mg/ml $_{DL}$-cysteine, 0.2 mg/mL bovine serum albumin and 1.6 U/mL papain, with the pH adjusted to 7.2 using 0.3 N NaOH. After several rinses in Hanks' solution, retinas were mechanically dissociated by gentle trituration with a glass pipette. The resulting cell suspension was plated onto culture dishes and cells were usually used for recordings within 5 h after dissociation.

Bipolar cells were identified based on their characteristic morphology (Karschin & Wässle 1990). Identification of dissociated rod and cone bipolar cells has been previously described (Pan 2000). In brief, rod bipolar cells had long and thick axons and usually retained axon terminals. Cone bipolar cells, on the other hand, had sparser dendritic trees and thinner axons, but their terminal varicosities were mostly absent.

HEK cell culture and DNA transfection

HEK-293 cells were maintained in Dulbecco's modified Eagle's medium (Gibco/BRL, Grand Island, NY) supplemented with 10% fetal bovine serum, 100 units/ml penicillin G and 100 μg/mL streptomycin at 37 °C in a humidified atmosphere of 95% air and 5% CO_2. For preparing DNA transfection, cells were seeded in 35 mm dishes, each with 3-5 × 10^4 counts. When the cells had reached 70% confluence, they were transfected with cDNA of rat α1G, human α1H, or rat α1I kindly provided by Dr. Perez-Reyes using Lipofectamine (Invitrogen, San Diego, CA) according to the manufacturer's instructions. All experiments were carried out 16-48 h

after transfection. Before recording, the culture medium was replaced with normal Hank's solution containing 2.5 mM Ca^{2+}.

Electrophysiological recordings

Recordings with patch electrodes in the whole-cell configuration were made using standard procedures (Hamill et al., 1981) at room temperature (20-25 °C) with an EPC-9 amplifier and PULSE software (Heka Electronik, Lambrecht/Pfalz, Germany). Electrodes were coated with silicone elastomer (Sylgard, Dow Corning, Midland, MI) and fire-polished. The resistance of the electrode was 7-14 MΩ. Series resistance ranged from 12 to 40 MΩ and was not compensated. Cell capacitance was cancelled and recorded using the PULSE software. Recordings were made either in the Hanks' solution (with 2.5 mM Ca^{2+}), described in the preceding text, or in high-Ca^{2+} (10 mM) extracellular solution containing (in mM): 95 NaCl, 5 KCl, 10 CsCl, 20 TEA-Cl, 1 $MgCl_2$, 10 $CaCl_2$, 5 HEPES, 22.2 glucose and 0.001% (v/v) phenol red, with the pH adjusted to 7.2. The electrode solution contained (in mM): 120 CsCl, 20 TEA-Cl, 1 $MgCl_2$, 0.5 $CaCl_2$, 5 EGTA, 10 HEPES, 0.5 Na-GTP and 2 Na-ATP, with the pH adjusted to 7.4 using CsOH. The electrode solution in the current clamp contained (in mM): 133 K-gluconate, 7 KCl, 1 $MgCl_2$, 0.5 $CaCl_2$, 5 EGTA, 10 HEPES, 0.5 Na-GTP and 2 Na-ATP, with the pH adjusted to 7.4 using KOH. Liquid junction potentials were corrected according to the procedure described by Neher (1992). Chemical agents were applied by local perfusion using gravity-driven superfusion pipettes placed ~200-300 μm away from the cell being recorded. The recording interval was 10 s, and only stable traces were used for analysis.

To examine voltage-gated Ca^{2+} currents, recordings were made in 10 mM Ca^{2+} extracellular solutions and voltage-activated K^+ currents were suppressed by the inclusion of Cs (10 mM) and tetraethylammonium (TEA) (10 mM) in the recording electrode and extracellular solutions. Bipolar cells were usually held at -80 mV and depolarized by a voltage ramp from -80 to +40 mV at a speed of 100 mV/second and by either a single 400-ms test pulse to -40 mV, or by a series of test pulses ranging from -60 to +40 mV. Some cone bipolar cells were also recorded in the current-clamp mode. In these cases, cells were first recorded in voltage-clamp mode at the holding potential of -80 mV. The recordings were then switched to current-clamp mode in which the amplifier delivered sufficient current to maintain the cell at the holding potential used in the voltage clamp.

Data were analyzed off-line using ORIGIN software (Microcal Software, Northampton, MA). The redox modulation, Ca^{2+}/Ba^{2+} permeability and Ni^{2+} inhibition of T-type currents were measured according to peak currents in response to the step pulse to -40 mV from a holding potential of -80 mV. Traces that could be repeated at least twice were deemed stable and were included in the analyses. Differences between groups were analyzed by one-way ANOVA, and P values < 0.05 were considered significant unless indicated otherwise. All data are presented as mean ± SD.

Chemicals

Drugs were applied by dissolving the drugs at known concentrations in the extracellular recording solutions. Ni^{2+} and Dithiothreitol (DTT) were prepared as 100 mM stocks in water, 5,5′-Dithio-bis(2-nitrobenzoic acid) (DTNB) as 100 mM stock and nimodipine as 10 mM stock in Dimethyl sulfoxide (DMSO). DMSO (0.5%) had no effects on Ca^{2+} currents when tested alone in isolated retinal bipolar cells or HEK cells transfected with Ca^{2+} channel subunit cDNAs. To test the relative permeability of Ba^{2+} versus Ca^{2+}, $CaCl_2$ (10 mM) was replaced by equal molar concentration of $BaCl_2$. In some recordings, 1 μM tetrodotoxin (TTX) was included in the extracellualr recording solutions to block possible voltage-gated Na^+ currents in cone bipolar cells. Mibefradil was a kind gift from F. Hoffmann (La Roche, Basel, Switzerland). All other chemicals were purchased from Sigma (St. Louis, MO).

Results

Expression patterns of T- and L-type Ca^{2+} currents in retinal cone bipolar cells

Two types of Ca^{2+} currents, T- and L-type, were observed in retinal cone bipolar cells from rats. Using voltage ramp stimulation, the T-type Ca^{2+} currents were activated at a membrane potential near -60 mV, and they reached their peak around -40 mV. In contrast, the L-type Ca^{2+} currents were activated at a higher membrane potential (near -40 to -30 mV), and they reached their peak around -20 or -10 mV (Fig. 1A). Based on the magnitude of T- and L-type currents we were able to distinguish three groups of cone bipolar cells. The first group showed prominent L-type currents with small or no apparent T-type current (n = 990; Fig. 1A). The second group displayed both prominent T- and L-type currents (n = 27; Fig. 1B), and the third group showed prominent T-type currents with small or no apparent L-type current (n = 783; Fig. 1C and D). Fig. 1E illustrates the amplitude of the T-type and L-type Ca^{2+} currents for all recorded cone bipolar cells. Most of the cone bipolar cells clearly fell into two groups: one with a prominent T-type Ca^{2+} current and the other with a prominent L-type Ca^{2+} current. For brevity, they will be referred to in this study as T-rich and L-rich cone bipolar cells, respectively. Conversely, cone bipolar cells that showed both prominent T- and L-type Ca^{2+} currents were rarely encountered. Most of these recordings were made from cells with a large number of surviving terminal varicosities or cells with their terminals still attached to tissue. This suggests that one of these two Ca^{2+} currents, T- or L-type, is located primarily in the terminals of cone bipolar cells. In addition, we noticed that if the retinas were treated in enzymatic solution for a longer period or if the recordings were performed after a longer waiting period following cell dissociation, we observed only cone bipolar cells with either T- or L-type Ca^{2+} current. This finding suggests that the small T- or L-type currents observed in the L- or T-rich cone bipolar cells, respectively, are vulnerable to cell dissociation or culturing.

In addition, the T-rich and L-rich cone bipolar cells appeared to have different sizes. Morphologically, the soma size of the L-rich cone bipolar cells appeared to be larger in general than that of the T-rich cone bipolar cells. Consistently, these two cell groups differed in whole-cell capacitance values. The T-rich cone bipolar cells had an average whole-cell capacitance of 2.2 ± 1.9 pF (n = 783). The L-rich group, on the other hand, had an average whole-cell capacitance of 3.1 ± 2.1 pF (n = 990). These two values were significantly different (one-way ANOVA, $P < 0.05$).

Three subgroups of T-rich cone bipolar cells with distinct T-type Ca^{2+} currents

Next we focused on characterizing the properties of T-type Ca^{2+} currents in the T-rich cone bipolar cells. The Ca^{2+} currents were evoked by step-wise test pulses so that both the magnitude and the kinetics of the current could be examined. The T-rich cone bipolar cells contained both T- and L-type Ca^{2+} currents, although the latter were small; the two types of current could be isolated from each other using a test pulse to -40 mV from a holding potential of -80 mV as a representative recording shown in Fig. 2A and B. First, a prominent T-type Ca^{2+} current was evident with the ramp stimulation (Fig. 2A). From the same cell, a fast transient current was elicited by the test pulse to -40 mV from a holding potential of -80 mV (dark trace in Fig. 2B). The current remained the same when BayK-8644, an L-type Ca^{2+} channel agonist, was applied (Fig. 2B). These results indicate that the test pulse to -40 mV from a holding potential of -80 mV did not significantly activate L-type Ca^{2+} currents in T-rich cone bipolar cells under our recording conditions.

Three Ca^{2+} channel α subunits, α1G, α1H, and α1I, are known to underlie the T-type Ca^{2+} currents (Perez-Reyes, 2003). Previous studies have reported distinct pharmacological and biophysical properties of T-type Ca^{2+} currents formed by these Ca^{2+} channel subunits (Cribbs et al., 1998; Lee et al., 1999; McRory et al., 2001; Todorovic et al., 2001). In particular, the

current due to the α1H subunit is sensitive to redox modulation (Cribbs et al., 1998; Todorovic et al., 2001). To determine if there is a differential expression of the α1H subunit among bipolar cells, we first examined the effects of redox agents on the T-type current in T-rich cone bipolar cells. We found that application of 2 mM dithiothreitol (DTT), a reducing agent, enhanced the T-type Ca^{2+} current in about one-third of cone bipolar cells in this group (see below). Modulation by DTT showed a fast onset and a relatively slow offset (Fig. 2C). No current desensitization was observed when the same concentration of DTT was repeatedly applied or when DTT was applied for up to 5 min ($n = 4$, data not shown). Conversely, application of 0.5 mM 5,5′-dithio-bis[2-nitrobenzoic acid] (DTNB), an oxidizing agent, reduced the T-type Ca^{2+} currents. The reduction of the current by DTNB could be reversed by subsequent application of DTT (Fig. 2D). Since redox modulation of T-type Ca^{2+} currents was observed in a portion of T-rich cone bipolar cells, this results suggests that a subgroup of T-rich cone bipolar cells expresses α1H T-type Ca^{2+} channels.

We further asked whether there is a differential expression of the three T-type Ca^{2+} channel subunits among cone bipolar cells. Since T-type Ca^{2+} channels of the three subunits are also known to differ in their Ca^{2+}/Ba^{2+} permeability and sensitivity to Ni^{2+} inhibition (McRory et al., 2001; Lee et al., 1999), we examined these properties of T-type currents in T-rich cone bipolar cells. Indeed, we found that T-rich cone bipolar cells could be divided into three subgroups based on the extent to which their T-type currents were sensitive to DTT modulation, permeable to Ca^{2+} versus Ba^{2+} and sensitive to Ni^{2+} inhibition.

The T-type Ca^{2+} current in the first subgroup was not significantly modulated by DTT (Fig. 3A). The T-type Ca^{2+} current after the application of DTT (2 mM) was reduced only by 4.2 ± 1.9% ($n = 44$) (also see Fig. 3J). The T-type currents in this same group were less permeable to Ba^{2+} than to Ca^{2+} (Fig. 3B). The peak currents were reduced to 75.5 ± 6.7% of the control ($n = 44$) when extracellular Ca^{2+} was replaced with Ba^{2+} (see Fig. 3J). Furthermore, the T-type Ca^{2+} current of this subgroup showed relatively low sensitivity to Ni^{2+} inhibition (Fig. 3C). Application of 20 μM Ni^{2+} reduced the current by 25.6 ± 6.0% ($n = 44$) (Fig. 3J).

The T-type Ca^{2+} current of the second subgroup of T-rich cone bipolar cells was sensitive to modulation by 2 mM DTT (Fig. 3D). The current was enhanced by 32.2 ± 8.2%, ($n = 29$) in the presence of 2 mM DTT (Fig. 3J). The current showed higher permeability to Ba^{2+} than to Ca^{2+} (Fig. 3E). The current increased to 145.2 ± 11% ($n = 29$) of the control (Fig. 3J) when Ca^{2+} was replaced with Ba^{2+}. In addition, the T-type Ca^{2+} current was highly sensitive to Ni^{2+} inhibition (Fig. 3F). Application of 20 μM Ni^{2+} reduced the current by 64 ± 11% ($n = 29$; Fig. 3J).

The T-type Ca^{2+} current of the third group was not significantly modulated by 2 mM DTT. The current was reduced by 3.4 ± 1.7% ($n = 20$; Fig. 3G) in the presence of 2 mM DTT. The current was equally permeable to Ca^{2+} and Ba^{2+} (Fig. 3H). The current only reduced to 99 ± 0.9 % ($n = 20$) of the control (Fig. 3J) when Ca^{2+} was replaced with Ba^{2+}. The current showed relatively low sensitivity to Ni^{2+} inhibition (Fig. 3I). Application of 20 μM Ni^{2+} reduced the current only by 22 ± 8.0 % (Fig. 3J).

In addition, the T-type Ca^{2+} current for the third subgroup showed the smallest amplitude among the three subgroup (30 ± 17 pA, $n = 20$). In contrast, the average values for the first and second subgroups were 76 ± 22 pA ($n = 44$) and 80 ± 17 pA ($n = 29$), respectively.

We also measured the activation and inactivation kinetics of the T-type Ca^{2+} currents in the three subgroups of cone bipolar cells because these properties have also been reported to differ among three T-type Ca^{2+} channel subunits (McRory et al. 2001). For this purpose, the time-to-peak values and decay time constant of the T-type Ca^{2+} currents were measured (Fig. 4A). The T-type Ca^{2+} current in the first subgroup had the fastest activation and inactivation among

the three subgroups. As shown in Fig. 4B and C, the average time-to-peak value and decay time constant were 19.5 ± 2.1 ms and 55.6 ± 3.8 ms (n = 44), respectively. For the T-type Ca^{2+} current in the second subgroup, the time-to-peak value and decay time constant were 24.7 ± 3.3 ms and 67.2 ± 6.2 ms (n = 29), respectively. The T-type Ca^{2+} current of the third subgroup had the slowest activation and inactivation kinetics; the time-to-peak value and decay time constant were 34.8 ± 3.7 ms and 93.5 ± 5.8 ms (n = 20), respectively.

Properties of T-type Ca^{2+} channel subunits in HEK cells

For a quantitative comparison between the properties of the T-type Ca^{2+} currents of three subgroups of cone bipolar cells and the recombinant T-type Ca^{2+} currents, we examined the pharmacological and biophysical properties of three cloned T-type subunits, α1G, α1H and α1I, in HEK cells under the same recording conditions. The representative recordings along with the average results for DTT modulation, Ca^{2+}/Ba^{2+} permeability, and Ni^{2+} sensitivity are shown in Fig. 5. The average values for the time peak and decay constants are shown in Fig. 6. The comparison of the data between three subgroups of cone bipolar cells and the three recombinant T-type Ca^{2+} subunits is shown in Table 1.

The results indicate that the overall properties of T-type Ca^{2+} currents in the three subgroups of cone bipolar cells resemble those of the α1G, α1H and α1I Ca^{2+} currents, respectively.

Properties of T-type Ca^{2+} current in rod bipolar cells

The T-type Ca^{2+} current in rod bipolar cells has been reported to show properties that are different from those of cone bipolar cells (Pan, 2000). We therefore examined the properties of T-type Ca^{2+} current in rod bipolar cells. We found that application of DTT did not significantly affect the current. The current in the presence of 2 mM DTT was increased only by 1.5 ± 1.8% (n = 15) (Fig. 7A and B). Consistent with previous findings (Pan, 2000), the current showed higher permeability to Ba^{2+} than to Ca^{2+} and relatively low sensitivity to Ni^{2+} inhibition (see Fig. 7A). The peak amplitude of the current increased by 53 ± 5.1% (n = 15) when Ca^{2+} was replaced with Ba^{2+}. Application of 20 μM Ni^{2+} reduced the current only by 22 ± 4.3% (n = 15; Fig. 7B). These results indicate that the T-type Ca^{2+} current in rod bipolar cells does not resemble any of the currents observed in cone bipolar cells.

Contribution of T- type Ca^{2+} currents to the voltage response in cone bipolar cells

In the CNS, T-type Ca^{2+} currents have been shown to play an important role in the generation of low-threshold spikes. To examine the possible functional role of T-type Ca^{2+} currents in T-rich cone bipolar cells, we examined the contribution of T-type Ca^{2+} currents to the voltage response of bipolar cells. The recordings were made in an extracellular solution containing 2.5 mM Ca^{2+} and without blocking K^+ channels. Under these recording conditions, prominent T-type Ca^{2+} currents were still observed by voltage ramp stimulation or by step pulse to -40 mV from a holding potential of -80 mV (Fig. 8A and B). The current was not affected by 1 μM TTX, indicating the absence of voltage-gated Na^+ current. In current-clamp recordings, stepwise current injections elicited regenerative membrane potentials in these cells. Fig. 8C shows a representative recording from a T-rich cone bipolar cell. The regenerative potentials showed a spike-like component on the top of the regenerative plateau potentials in an all-or-nothing manner. The spike-like regenerative potentials persisted in the presence of 1 μM TTX (data not shown), confirming that voltage-gated Na^+ channels were not involved. Conversely, application of 10 μM mibefradil, a T-type Ca^{2+} channel antagonist, blocked the spike-like component but not the regenerative plateau potentials (Fig. 8D). Similar results were observed in other T-rich cone bipolar cells (n = 25).

Discussion

Two broad groups of isolated cone bipolar cells

The results of this study have shown that based on the expression pattern of T- and L-type Ca^{2+} currents, two broad groups of retinal cone bipolar cells exist in rats. We also recorded 210 isolated cone bipolar cells from mouse retinas. Similarly, two groups of cone bipolar cells were observed based on the expression of T- and L-type Ca^{2+} currents (data not shown). One broad group of cone bipolar cells, referred to as T-rich cone bipolar cells, shows prominent T-type Ca^{2+} currents, whereas the second group, referred to as L-rich cone bipolar cells, shows prominent L-type currents. It should be emphasized that most of the distal dendrites and terminal varicosities of cone bipolar cells in our preparation were lost during the cell dissociation (Pan, 2000). Therefore, the Ca^{2+} currents observed under our conditions should primarily originate in the soma. In addition, we did not notice a correlation between the T-rich or L-rich cone bipolar cells and the extent of surviving dendrites and axon terminals. Therefore, the observation of T-rich and L-rich cone bipolar cells should not be due to variation in the intactness of axon terminals and/or dendrites. Rather, our results suggest that there are two groups of cone bipolar cells, with each predominantly expressing either T-type or L-type Ca^{2+} channels in their somata.

It should also be noted that the T- and L-rich cone bipolar cells usually displayed small L- and T-type Ca^{2+} currents, respectively. Interestingly, these small T- or L-type currents were vulnerable to cell dissociation or culturing. Since the distal dendrites and/or axon terminals might more easily deteriorate during long enzyme exposure or cell culture, these small T- and L-type currents might be located in the distal dendrites and/or axon terminals. This interpretation is consistent with the observation that the group of cone bipolar cells that displayed both large T- and L-type Ca^{2+} currents usually had relatively intact axon terminals. Our results suggest that in L-rich cone bipolar cells, the T-type Ca^{2+} channels are located primarily in distal dendrites and/or axon terminals, whereas in T-rich cone bipolar cells, the L-type Ca^{2+} channels are located primarily in distal dendrites and/or axon terminals. Taken together, our results suggest a differential distribution of T- and L-type Ca^{2+} channels in the two broad groups of cone bipolar cells.

For rod bipolar cells in the rat and mouse, previous studies have shown that the L-type Ca^{2+} channels localize to the axon terminals (Hartveit, 1997; de la Villa, et al., 1998; Pan, 2000), whereas T-type Ca^{2+} channels are located both in the soma and at axon terminals (Pan et al., 2001). Since isolated rod bipolar cells display prominent T-type Ca^{2+} currents (Pan, 2000), rod bipolar cells therefore belong to the T-rich group.

In addition, we found that the T-rich and L-rich cone bipolar cells appeared to have different somatic sizes based on their morphological appearance and their whole-cell capacitance. The T-rich cone bipolar cells were generally smaller in size than the L-rich cone bipolar cells. At least nine types of cone bipolar cells have been classified in the mammalian retina based on their terminal stratification in the interplexiform layer (Euler and Wässle, 1995; Hartveit, 1997). Cone bipolar cells are further divided into ON- and OFF-types on the basis of their polarity in response to light (Werblin and Dowling, 1969). Furthermore, the sustained and transient responses in the retina have been reported to originate, in part, in bipolar cells (Awatramani & Slaughter, 2000). It would be interesting for future studies to determine whether these two groups of bipolar cells correspond to different functional types of cone bipolar cells.

Three subgroups of T-rich cone bipolar cells with distinct T-type Ca^{2+} currents

We have also shown that T-rich cone bipolar cells can be divided into three subgroups based on pharmacological and biophysical properties of their T-type currents: redox modulation, permeability of Ca^{2+} versus Ba^{2+}, and sensitivity to Ni^{2+} inhibition. Notably, these properties of the T-type currents in these three subgroups of cone bipolar cells were found to closely resemble those of the recombinant T-type Ca^{2+} currents of α1G, α1H, and α1I, respectively, as previously reported in HEK cells (Todorovic et al., 2001; McRory et al. 2001; Lee et al., 1999) and confirmed in this study. Furthermore, the activation kinetics of the T-type Ca^{2+} currents observed among these three subgroups also largely resembled those of the three recombinant Ca^{2+} channel subunits (McRory et al., 2001). However, the decay time constants of the T-type Ca^{2+} currents in the three subgroups of cone bipolar cells were found to be substantially longer than those of their corresponding recombinant Ca^{2+} channel currents. This discrepancy might arise from the presence of accessory subunits (Hobom et al., 2000), alternative splicing (Murbartian et al., 2002), or possible posttranslational modifications of the T-type Ca^{2+} channels in bipolar cells (Chemin et al., 2006). Nevertheless, our results suggest that each subgroup of T-rich cone bipolar cells predominantly expresses a single subunit of the T-type Ca^{2+} channel in the soma. Interestingly, there is a similar finding in pain pathways, where one type of small-size spinal dorsal root ganglion cells (T-rich) expresses primarily the α1H subunit (Talley et al., 1999; Jevtovic-Todorovic & Todorovic, 2006).

As mentioned above, rod bipolar cells belong to the T-rich cell group. Interestingly, the properties of T-type Ca^{2+} currents in rod bipolar cells did not fully match those of any of the recombinant T-type Ca^{2+} channel subunits. Comparing the properties of Ca^{2+} currents in rod bipolar cells with those of the three recombinant T-type Ca^{2+} channel subunits, however, suggests that the properties of the Ca^{2+} currents in rod bipolar cells more closely resemble those of the recombinant (1I subunit than other subunits. In particular, activation and inactivation of the T-type Ca2+ current in rod bipolar cells are extremely slow (Pan, 2000), a marked property of the (1I Ca2+ current (Monteil et al., 2000; McRory et al., 2001). The only major discrepancy between the Ca2+ current of rod bipolar cells and (1I Ca2+ current is the Ba2+/Ca2+ permeability: the current in rod bipolar cells is more permeable to Ba2+ than to Ca2+, while the (1I Ca2+ channel is equally permeable to Ca2+ and Ba2+. To date, only three T-type Ca2+ channel genes have been cloned, but multiple splicing variants of these subunits have been reported (Perez-Reyes, 2003). A recent study identified certain charged amino acid residues in T-type Ca2+ channels that could influence the divalent cation selectivity (Cens et al., 2007). Therefore, the atypical properties of the T-type Ca2+ current in rod bipolar cells may arise from a splicing variant or mutant of the (1I Ca2+ channel. It is also possible that the properties of the T-type Ca2+ channel in rod bipolar cells are altered by the presence of accessory subunits or posttranslational modifications.

Implications for T-type calcium channel functions in bipolar cells

One of the important functions of T-type Ca^{2+} channels in the CNS is to support the generation of low-threshold Ca^{2+} spikes (LTSs). LTSs are usually generated in the dendrites and propagated through the whole cell membrane, thus activating high-threshold spikes that are mediated by L-type Ca^{2+} channels (Huguenard 1998; Bobkov & Ache, 2007; Jevtovic-Todorovic & Todorovic, 2006). T-type Ca^{2+} currents were previously shown to be essential for the initiation of the spontaneous activity in bipolar cells *in vitro* (Ma & Pan, 2003). As shown in this study, regenerative spike-like potentials mediated by the T-type Ca^{2+} current could occur in T-rich cone bipolar cells. Interestingly, after the blockade of T-type Ca^{2+} current, regenerative plateau potentials were still present (see Fig. 8D). Regenerative action potentials mediated by L-type Ca^{2+} channels have been reported in bipolar cells of goldfish (Protti et al., 2000). Therefore, it is possible that the interplay of T- and L-type Ca^{2+} channels may also shape the waveform of mammalian bipolar cells.

Furthermore, this study shows the existence of three subgroups of T-rich cone bipolar cells. Each subgroup predominantly expresses a single type of T-type Ca^{2+} channel subunit in their somata, while rod bipolar cells express an atypical T-type Ca^{2+} channel. Therefore, bipolar cells of different types could express T-type Ca^{2+} channels with different activation and inactivation kinetics. In addition, the function of these different T-type Ca^{2+} channels could be subjected to the regulation by endogenous substances (Nelson et al., 2007; Hildebrand et al., 2007; Chemin et al., 2006). Furthermore, previous studies showed that the activation of T-type Ca^{2+} channels at the axon terminal of bipolar cells could trigger transmitter release (Pan et al., 2001; Singer & Diamond, 2003). Together, the differential expression of multiple T-type Ca^{2+} channels may contribute to the diverse signal processing of bipolar cells.

The functional significance of T-type Ca^{2+} channels in bipolar cells would be dependent on the membrane potential range of the bipolar cells. The true membrane potential range of bipolar cells *in vivo* remains unclear. The dark membrane potentials of mammalian bipolar cells were reported to be in the range of −60 mV to −25 mV (Kaneko et al., 1989; Karschin & Wässle, 1990; Gillette & Dacheux, 1995; Berntson & Taylor, 2000; Euler & Masland, 2000). A wider range has been reported in lower vertebrates (Tessier-Lavigne et al., 1988; Connaughton & Maguire, 1998). The operating range of the membrane potential of a bipolar cell would be dependent on light conditions and the functional type of the bipolar cell, ON versus OFF. In addition, the operating range could be subject to modulation by neurotransmitters (Lukasiewicz & Werblin, 1994; Pan & Lipton, 1995; Euler & Wässle, 1998; Cui et al., 2003) or neuromodulators (Yu et al., 2008) or influenced by the membrane potential of other neurons through gap junctions (Xin & Bloomfield, 1999; Trexler et al., 2001). It is possible that under certain conditions, the membrane potential of certain bipolar cells may operate over a range in which a significant portion of T-type Ca^{2+} channels are activated (Pan, 2000). It is worth pointing out here that certain types of retinal cone bipolar cells express voltage-dependent Na^{+} channels, which also require a relatively negative membrane potential for function. Na^{+} channels in retinal bipolar cells have been shown to play a functional role in retinal information processing (Ichinose *et al.*, 2005; Ichinose & Lukasiewicz, 2007; Mojumder *et al.*, 2008). Thus, it will be of interest for future studies to investigate the functional role of the differential expression of multiple T-type Ca^{2+} channels in retinal bipolar cells.

Acknowledgments

We would like to thank Dr. E. Perez-Reyes for providing us the recombinant α1G, α1H, and α1I Ca^{2+} channel subunits. This research was supported by NIH grant EY12180 (Z-H Pan) and core grant EY04068 to the Department of Anatomy and Cell Biology at Wayne State University.

References

Awatramani GB, Slaughter MM. Origin of transient and sustained responses in ganglion cells of the retina. Journal of Neuroscienc 2000;20:7087–7095.

Berntson A, Taylor WR. Response characteristics and receptive field widths of on-bipolar cells in the mouse retina. Journal of Physiology (London) 2000;524:879–89. [PubMed: 10790165]

Bobkov YV, Ache BW. Intrinsically bursting olfactory receptor neurons. Journal of Neurophysiolog 2007;97:1052–1057.

Burrone J, Lagnado L. Electrical resonance and Ca^{2+} influx in the synaptic terminal of depolarizing bipolar cells from the goldfish retina. Journal of Physiology (London) 1997;505:571–584. [PubMed: 9457636]

Cens T, Rousset M, Kajava A, Charnet P. Molecular determinant for specific Ca/Ba selectivity profiles of low and high threshold Ca^{2+} channels. Journal of General Physiology 2007;130:415–425. [PubMed: 17893194]

Chemin J, Traboulsie A, Lory P. Molecular pathways underlying the modulation of T-type calcium channels by neurotransmitters and hormones. Cell Calcium 2006;40:121–134. [PubMed: 16797700]

Connaughton VP, Maguire G. Differential expression of voltage-gated K^+ and Ca^{2+} currents in bipolar cells in the zebrafish retinal slice. European Journal of Neuroscience 1998;10:1350–1362. [PubMed: 9749789]

Cribbs LL, Lee J, Yang J, Satin J, Zhang Y, Daud A, Barcley J, Williamson MP, Fox M, Rees M, Perez-Reyes E. Cloning and characterization of α1H from human heart, a member of the T-type Ca^{2+} channel gene family. Circulation Research 1998;83:103–109. [PubMed: 9670923]

Cui J, Ma YP, Lipton SA, Pan ZH. Glycine receptors and glycinergic synaptic input at the axon terminals of mammalian retinal rod bipolar cells. Journal of Physiology (London) 2003;553:895–909. [PubMed: 14514876]

de la Villa P, Vaquero CF, Kaneko A. Two types of Ca^{2+} currents of the mouse bipolar cells recorded in the retinal slice preparation. European Journal of Neuroscience 1998;10:317–323. [PubMed: 9753140]

Euler T, Masland SH. Light-evoked responses of bipolar cells in a mammalian retina. Journal of Neurophysiology 2000;83:1817–1829. [PubMed: 10758094]

Euler T, Wässle H. Immunocytochemical identification of cone bipolar cells in the rat retina. Journal of Comparative Neurology 1995;361:461–478. [PubMed: 8550893]

Euler T, Wässle H. Different contributions of $GABA_A$ and $GABA_C$ receptors to rod and cone bipolar cells in a rat retinal slice preparation. Journal of Neurophysiology 1998;79:1384–1395. [PubMed: 9497419]

Gillette MA, Dacheux RF. GABA- and glycine-activated currents in the rod bipolar cell of the rabbit retina. Journal of Neurophysiology 1995;74:856–875. [PubMed: 7472389]

Hamill OP, Marty A, Neher E, Sakmann B, Sigworth FJ. Improved patch-clamp techniques for high-resolution current recording from cells and cell-free membrane patches. Pflügers Archiv 1981;391:85–100.

Hartveit E. Functional organization of cone bipolar cells in the rat retina. Journal of Neurophysiolog 1997;77:1716–1730.

Heidelberger R, Matthews G. Calcium influx and calcium current in single synaptic terminals of goldfish retinal bipolar neurons. Journal of Physiology (London) 1992;447:235–256. [PubMed: 1317429]

Hildebrand ME, David LS, Hamid Jawed, Mulatz K, Garcia E, Zamponi GW, Snutch TP. Selective inhibition of $Ca_v3.3$ T-type calcium channels by $G_{q/11}$-coupled muscarinic acetylcholine receptors. Journal of Biological Chemistry 2007;282:21043–21055. [PubMed: 17535809]

Hobom M, Dai S, Marais E, Lacinova L, Hofmann F, Klugbauer N. Neuronal distribution and functional characterization of the calcium channel α2-δ2 subunit. European Journal of Neuroscience 2000;12:1217–1226. [PubMed: 10762351]

Huguenard JR. Low-voltage-activated (T-type) calcium-channel genes identified. Trends in Neurosciences 1998;21:451–452. [PubMed: 9829683]

Ichinose T, Shields CR, Lukasiewicz PD. Na^+ channels in transient retinal bipolar cells enhance visual responses in ganglion cells. Journal of Neuroscience 2005;25:1856–1865. [PubMed: 15716422]

Ichinose T, Lukasiewicz PD. Ambient light regulates Na^+ channel activity to dynamically control retinal signaling. Journal of Neuroscience 2007;27:4756–4764. [PubMed: 17460088]

Jevtovic-Todorovic V, Todorovic SM. The role of peripheral T-type calcium channels in pain transmission. Cell Calcium 2006;40:197–203. [PubMed: 16777222]

Kaneko A, Pinto LH, Tachibana M. Transient calcium current of retinal bipolar cells of the mouse. Journal of Physiology (London) 1989;410:613–629. [PubMed: 2552084]

Kaneko A, Suzuki S, Pinto LH, Tachibana M. Membrane currents and pharmacology of retinal bipolar cells: a comparative study on goldfish and mouse. Comparative Biochemistry and Physiology 1991;98:115–127. [PubMed: 2060275]

Karschin A, Wässle H. Voltage- and transmitter-gated currents in isolated rod bipolar cells of rat retina. Journal of Neurophysiolog 1990;63:860–876.

Lacinova L, Klugbauer N, Hofmann F. Low voltage activated calcium channels: from genes to function. General Physiology and Biophysics 2000;19:121–136. [PubMed: 11156438]

Lee JH, Gomora JC, Cribbs LL, Perez-Reyes E. Nickel block of three cloned T-type calcium channels: low concentrations selectively block alpha1H. Biophysical Journal 1999;77:3034–3042. [PubMed: 10585925]

Lukasiewicz PD, Werblin FS. A novel GABA receptor modulates synaptic transmission from bipolar to ganglion and amacrine cells in the tiger salamander retina. Journal of Neuroscience 1994;14:1213–1223. [PubMed: 7907138]

Ma YP, Pan ZH. Spontaneous regenerative activity in mammalian retinal bipolar cells: roles of multiple subtypes of voltage-dependent Ca^{2+} channels. Visual Neuroscience 2003;20:131–139. [PubMed: 12916735]

Ma YP, Cui JJ, Pan ZH. Heterogeneous expression of voltage-dependent Na^{+} and K^{+} channels in mammalian retinal bipolar cells. Visual Neuroscience 2005;22:119–133. [PubMed: 15935105]

Mao BQ, MacLeish PR, Victor JD. The intrinsic dynamics of retinal bipolar cells isolated from tiger salamander. Visual Neuroscienc 1998;15:425–438.

McRory JE, Santi CM, Hamming KS, Mezeyova J, Sutton KG, Baillie DL, Stea A, Snutch TP. Molecular and functional characterization of a family of rat brain T-type calcium channels. Journal of Biological Chemistry 2001;276:3999–4011. [PubMed: 11073957]

Maguire G, Maple B, Lukasiewicz P, Werblin F. Amino butyrate type B receptor modulation of L-type calcium channel current at bipolar cell terminals in the retina of the tiger salamander. Proceedings of the National Academy of Sciences USA 1989;86:10144–10147.

Mojumder DK, Sherry DM, Frishman LJ. Contribution of voltage-gated sodium channels to the b-wave of the mammalian flash electroretinogram. Journal of Physiology (London) 2008;586:2551–2580. [PubMed: 18388140]

Monteil A, Chemin J, Leuranguer V, Altier C, Mennessier G, Bourinet E, Lory P, Nargeot J. Specific properties of T-type calcium channels generated by the human alpha 1I subunit. Journal of Biological Chemistry 2000;275:16530–16535. [PubMed: 10749850]

Murbartian J, Arias JM, Lee JH, Gomora JC, Perez-Reyes E. Alternative splicing of the rat Ca(v)3.3 T-type calcium channel gene produces variants with distinct functional properties. FEBS Letter 2002;528:272–278.

Neher E. Correction for liquid junction potentials in patch clamp experiments. Methods in Enzymology 1992;207:123–131. [PubMed: 1528115]FEBS Letter

Nelson MT, Joksovic PM, Su P, Kang HW, Deusen AV, Baumgart JP, David LS, Snutch TP, Barrett PQ, Lee JH, Zorumski CF, Perez-Reyes E, Todorovic MS. Molecular Mechanisms of Subtype-Specific Inhibition of Neuronal T-Type Calcium Channels by Ascorbate. Journal of Neuroscience 2007;27:12577–12583. [PubMed: 18003836]

Pan ZH. Differential expression of high- and two types of low-voltage-activated calcium currents in rod and cone bipolar cells of the rat retina. Journal of Neurophysiolog 2000;83:513–527.

Pan ZH, Hu HJ, Perring P, Andrade R. T-Type Ca^{2+} Channels Mediate Neurotransmitter Release in Retinal Bipolar Cells. Neuron 2001;32:89–98. [PubMed: 11604141]

Pan ZH, Lipton SA. Multiple GABA receptor subtypes mediate inhibition of calcium responses at rat retinal bipolar cell terminals. Journal of Neuroscience 1995;15:2668–2679. [PubMed: 7722621]

Perez-Reyes E. Molecular physiology of low-voltage-activated T-type calcium channels. Physiological Reviews 2003;83:117–161. [PubMed: 12506128]

Perez-Reyes E, Cribbs LL, Daud A, Lacerda AE, Barclay J, Williamson MP, Fox M, Rees M, Lee JH. Molecular characterization of a neuronal low-voltage-activated T-type calcium channel. Nature 1998;391:896–900. [PubMed: 9495342]

Protti DA, Flores-Herr N, von Gersdorff H. Light evokes Ca^{2+} spikes in the axon terminal of a retinal bipolar cell. Neuron 2000;25:215–227. [PubMed: 10707985]

Protti DA, Llano I. Calcium currents and calcium signaling in rod bipolar cells of rat retinal slices. Journal of Neuroscience 1998;18:3715–3724. [PubMed: 9570802]

Satoh H, Aoki K, Watanabe SI, Kaneko A. L-type calcium channels in the axon terminal of mouse bipolar cells. Neuroreport 1998;9:2161–2165. [PubMed: 9694192]

Singer JH, Diamond JS. Sustained $Ca2^{+}$ entry elicits transient postsynaptic currents at a retinal ribbon synapse. Journal of Neuroscience 2003;23:10923–10933. [PubMed: 14645488]

Tachibana M, Okada T, Arimura T, Kobayashi K. Dihydropyridine-sensitive calcium current mediates neurotransmitter release from retinal bipolar cells. Annual New York Academy of Sciences 1993;707:359–361.

Talley EM, Cribbs LL, Lee JH, Daud A, Perez-Reyes E, Bayliss DA. Differential distribution of three members of a gene family encoding low voltage-activated (T-type) calcium channels. Journal of Neuroscience 1999;19:1895–1911. [PubMed: 10066243]

Tessier-Lavigne M, Attwell D, Mobbs P, Wilson M. Membrane current in retinal bipolar cells of the axolotl. Journal of General Physiology 1988;91:49–72. [PubMed: 3125305]

Todorovic SM, Jevtovic-Todorovic V, Meyenburg A, Mennerick S, Perez-Reyes E, Romano C, Olney JW, Zorumski CF. Redox modulation of T-type calcium channels in rat peripheral nociceptors. Neuron 2001;31:75–85. [PubMed: 11498052]

Trexler EB, Li W, Mills SL, Massey SC. Coupling from AII amacrine cells to ON cone bipolar cells is bidirectional. Journal of Comparative Neurology 2001;437:408–422. [PubMed: 11503143]

Wässle H. Parallel processing in the mammalian retina. Nature Reviews Neuroscience 2004;5:747–757.

Werblin FS, Dowling JE. Organization of the retina of the mudpuppy, Necturus maculosus. II. Intracellular recording. Journal of Neurophysiology 1969;32:39–55.

Wu SM, Gao F, Maple BR. Functional architecture of synapses in the inner retina: segregation of visual signals by stratification of bipolar cell axon terminals. Journal of Neuroscience 2000;20:4462–4470. [PubMed: 10844015]

Xin D, Bloomfield SA. Comparison of the responses of AII amacrine cells in the dark- and light-adapted rabbit retina. Visual Neuroscience 1999;16:653–665. [PubMed: 10431914]

Yu Y, Satoh H, Wu SM, Marshak DW. Histamine enhances voltage-gated potassium currents of ON bipolar cells in macaque retina. Investigative Ophthalmology and Visual Science 2008;50:959–965. [PubMed: 18836167]

Zenisek D, Matthews G. Calcium action potentials in retinal bipolar neurons. Visual Neuroscience 1998;15:69–75. [PubMed: 9456506]

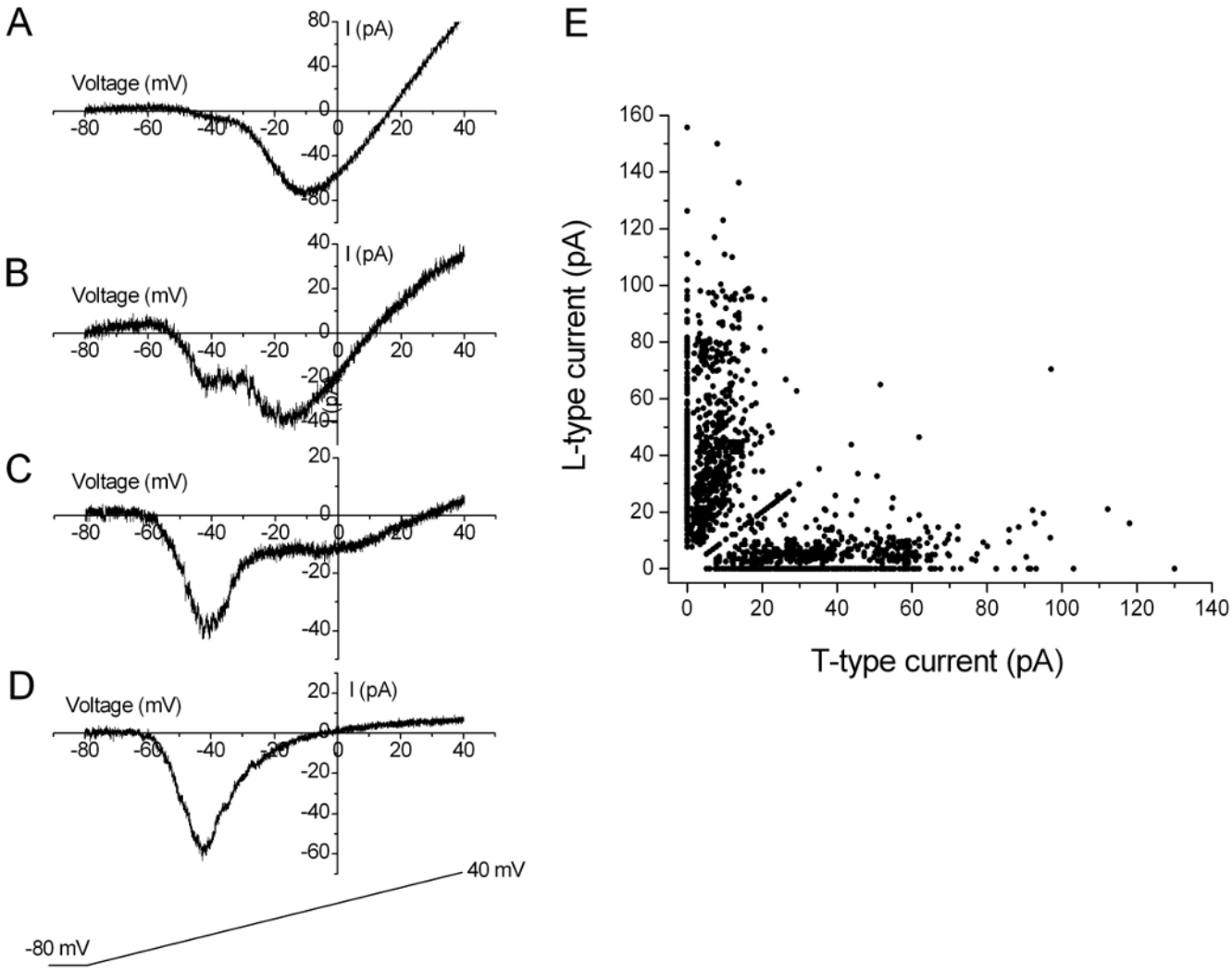

Figure 1. Profile of T- and L-type Ca^{2+} currents of isolated cone bipolar cells

Two peak-inward Ca^{2+} currents (T- and L-type) were evoked in response to stimulation in which the voltage was ramped up to +40 mV from a holding potential of −80 mV. Three groups of cone bipolar cells were observed based on the amplitudes of T- and L-type Ca^{2+} currents. (A) Cone bipolar cells displaying primarily L-type Ca^{2+} currents. (B) cone bipolar cells displaying prominent T- and L-type Ca^{2+} currents. (C and D) cone bipolar cells displaying primarily T-type Ca^{2+} currents; E: distribution plot of T- and L-type currents in cone bipolar cells (n = 1800).

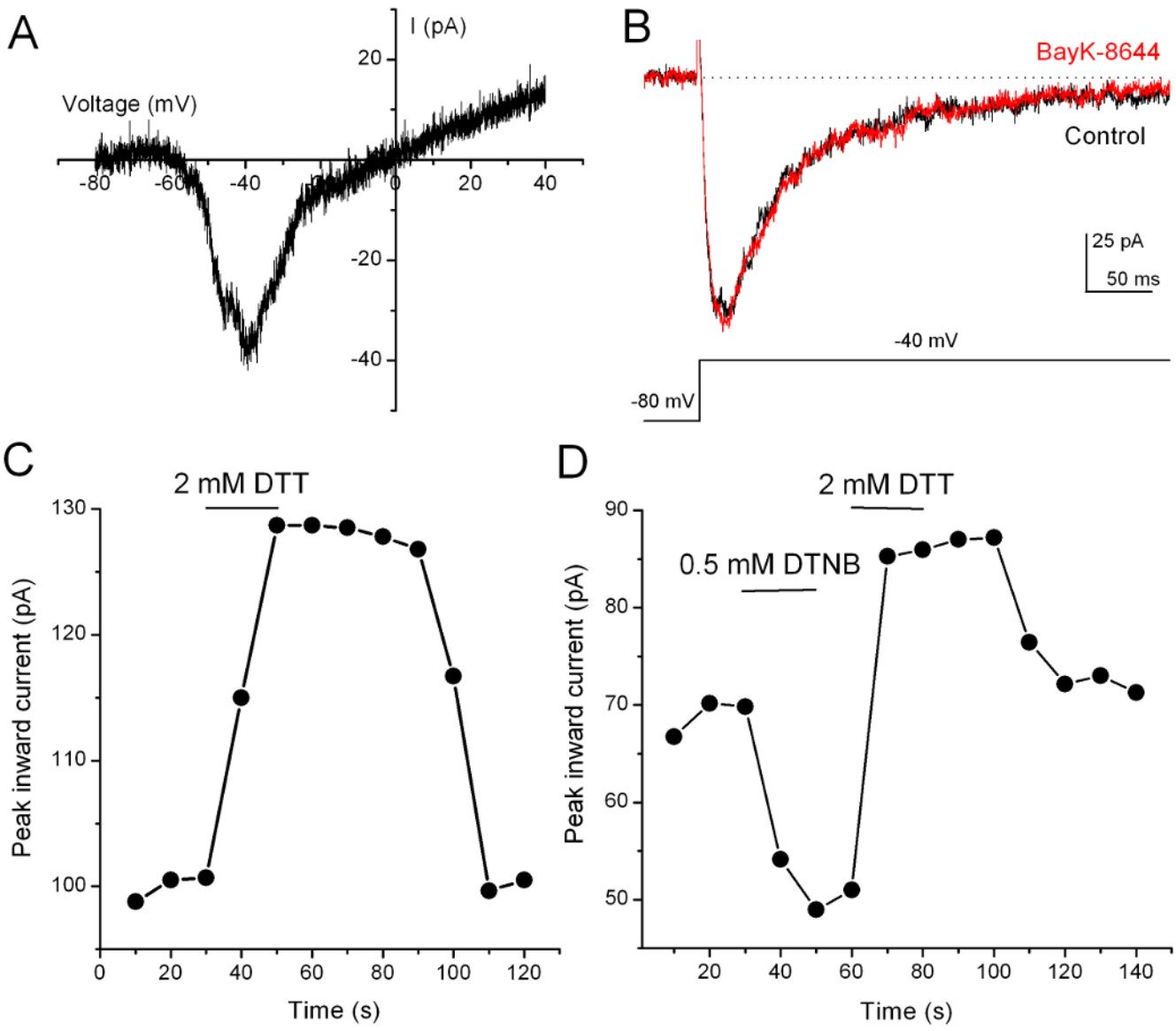

Figure 2. Redox modulation of T-type Ca^{2+} current in some T-rich cone bipolar cells

(A) A representative recording of T-type Ca^{2+} currents form T-rich cone bipolar cells evoked by a voltage ramp to +40 mV from a holding potential of −80 mV. (B) Currents evoked by a voltage step pulse to −40 mV from a holding potential of −80 mV did not increase in the presence of 1 μM BayK-8644. (C) Application of DTT increased the peak T-type Ca^{2+} current, which had a fast onset and a relatively slow offset. (D) Application of DTNB decreased the peak T-type Ca^{2+} current. The effect of DTNB could be quickly reversed by DTT. The T-type currents were evoked by step pulses to -40 mV from a holding potential of -80 mV.

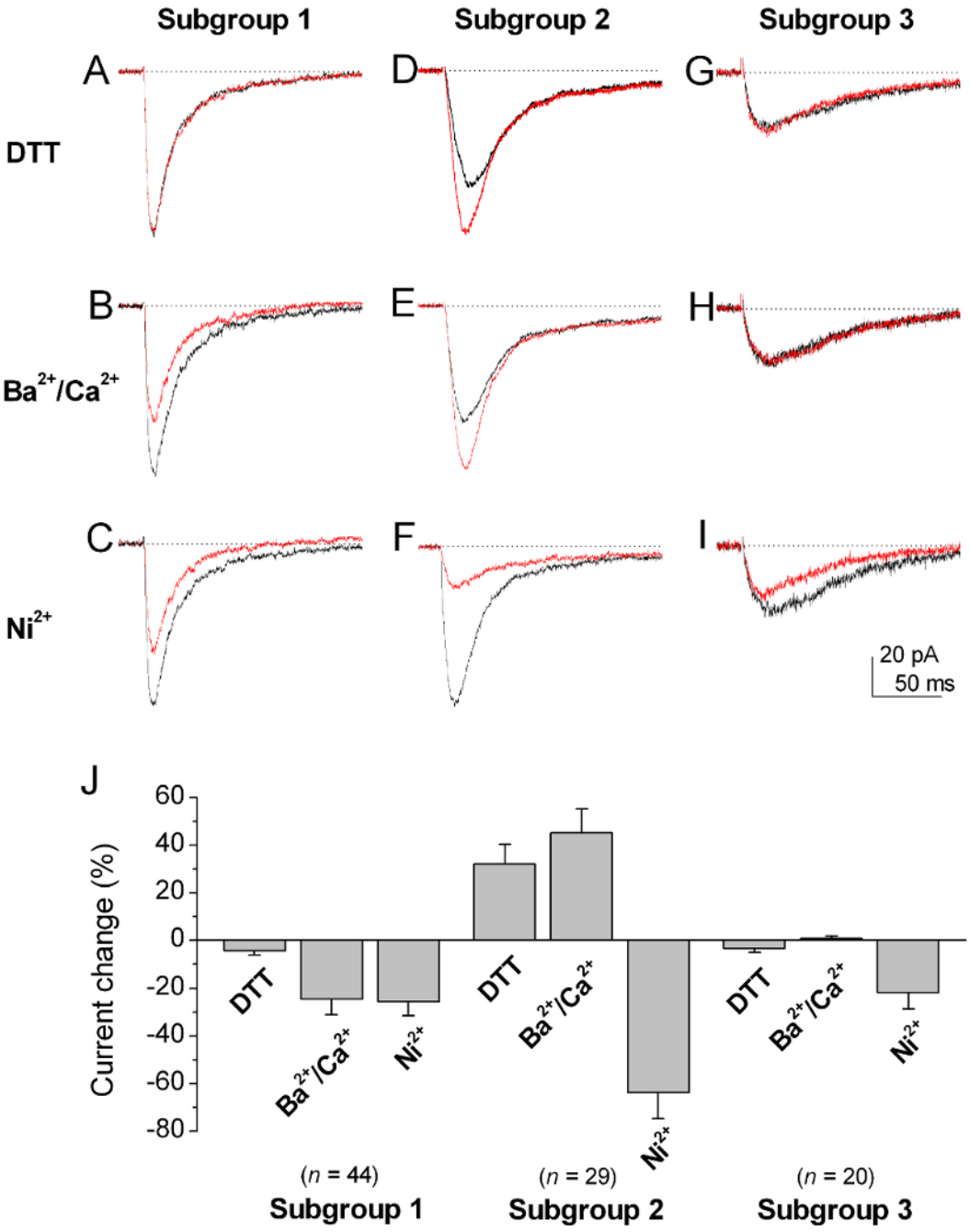

Figure 3. Comparison of the properties of redox modulation, permeability for Ca^{2+} versus Ba^{2+}, and Ni^{2+} inhibition of T-type Ca^{2+} currents among three subgroups of T-rich cone bipolar cells

Currents were evoked by a voltage step pulse to -40 mV from a holding potential of -80 mV. Three subgroups of cone bipolar cells were observed based on the extent to which their T-type Ca^{2+} currents were sensitive to modulation by 2 mM DTT, were permeable to Ca^{2+} versus Ba^{2+}, and were sensitive to 20 μM Ni^{2+}. (A-C) The T-type Ca^{2+} currents in the first subgroup did not show significant DTT modulation (A), they were less permeable to Ba^{2+} than to Ca^{2+} (B) and they showed low sensitivity to Ni^{2+} inhibition (C). (D-F) The T-type Ca^{2+} currents in the second subgroup were potentiated by DTT (D). In addition, they were more permeable to Ba^{2+} than to Ca^{2+} (E), and they were more sensitive to Ni^{2+} inhibition (F). (G-I) The T-type

currents in the third subgroup did not show significant modulation by DTT, they were equally permeable to Ca^{2+} and Ba^{2+}, and they had low sensitivity to Ni^{2+} inhibition. (J) The bar graphs are the sums of the percentage changes to control of T-type currents in DTT modulation, permeability to Ca^{2+} versus Ba^{2+}, and Ni^{2+} inhibition in three subgroups of cone bipolar cells. The T-type currents in the second subgroup of cone bipolar cells were significantly more sensitive to Ni^{2+} inhibition than those of the other two subgroups ($p < 0.05$). Error bars indicate the SD.

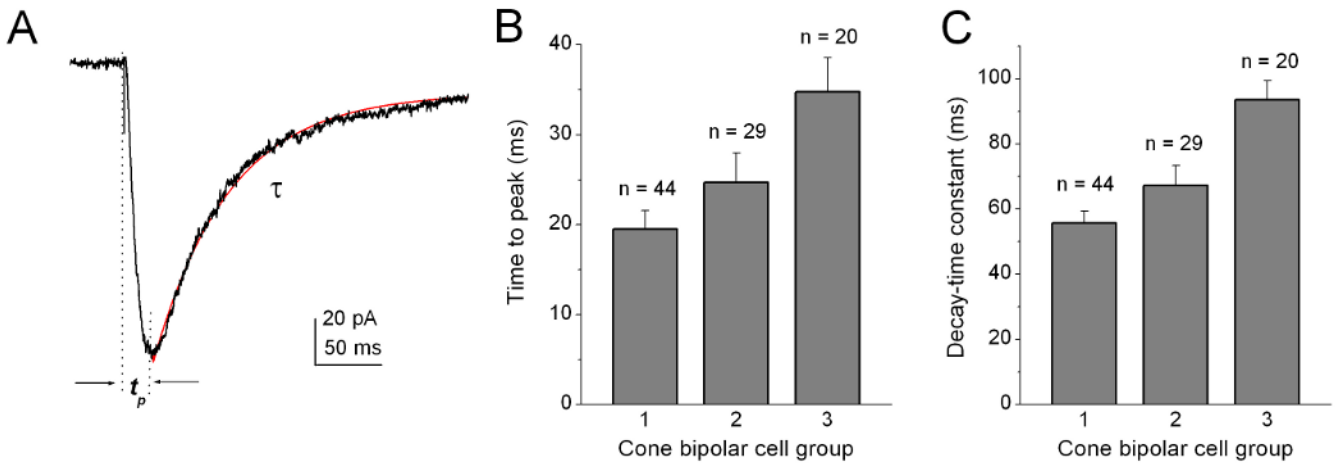

Figure 4. Comparison of the kinetic properties of T-type currents among three subgroups of isolated T-rich cone bipolar cells

(A) Typical recording of T-type currents in T-rich cone bipolar cells and measurement of time-to-peak (t_p) values and the inactivation time constant (τ). The currents were evoked by a voltage pulse to −40 mV from a holding potential of -80 mV in the presence of 10 mM Ca^{2+}. (B) Average time-to-peak value and inactivation time constant of T-type Ca^{2+} currents recorded from the three subgroups of T-rich cone bipolar cells. Error bars indicate the SD.

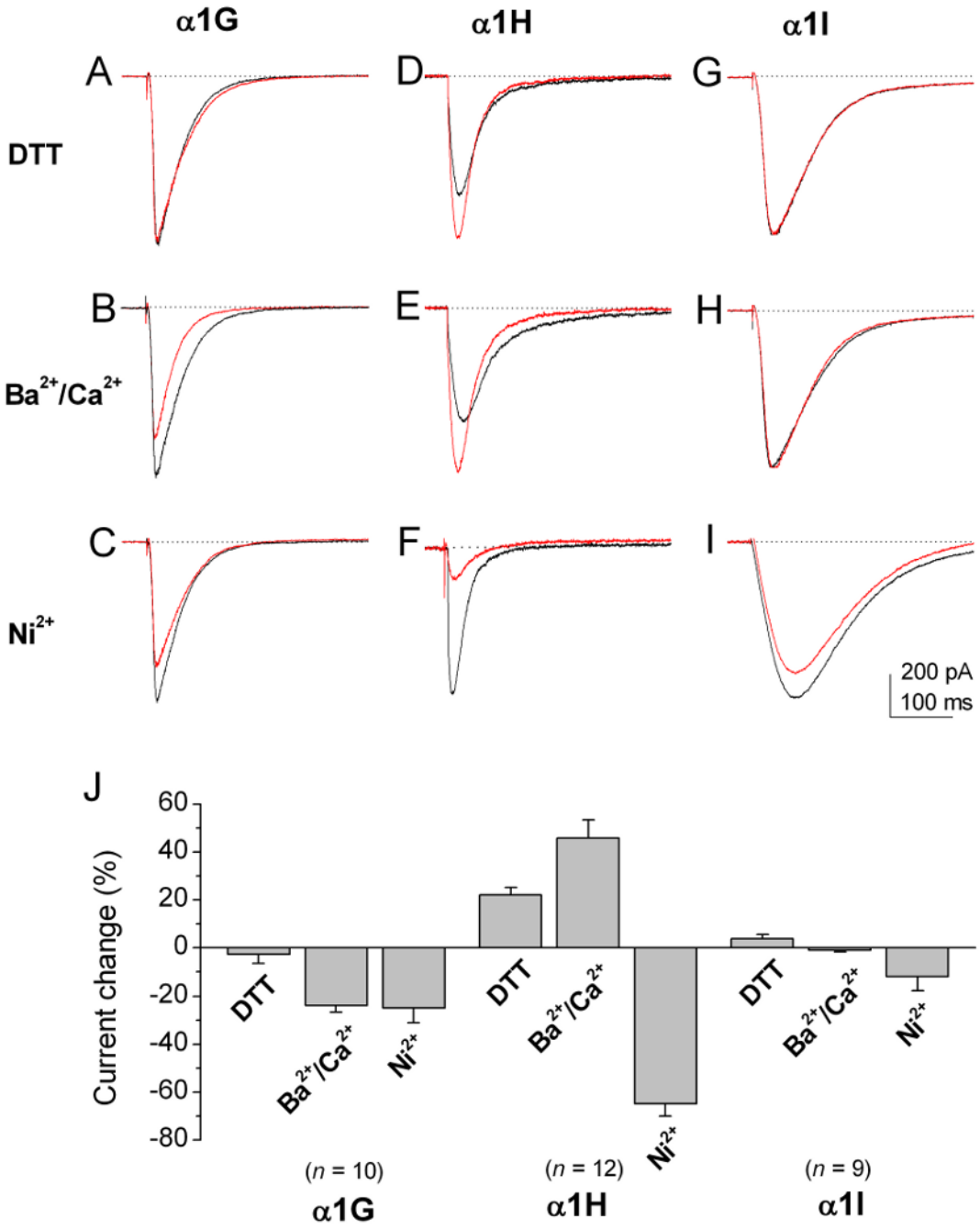

Figure 5. The properties of Ca^{2+} currents recorded from HEK-293 cells transiently expressing α1G, α1H, or α1I Ca^{2+} channel subunits

Currents were evoked by a voltage pulse to -40 mV from a holding potential of −80 mV. (A-C) α1G currents did not show significant DTT modulation (A), they were less permeable to Ba^{2+} than to Ca^{2+} (B) and they had relatively low sensitivity to 20 μM Ni^{2+} inhibition. (D-F) α1H currents were potentiated by DTT (D). They were more permeable to Ba^{2+} than to Ca^{2+} (E) and more sensitive to 20 μM Ni^{2+} inhibition (F). (G-I) α1I currents did not show significant DTT modulation (G), they were equally permeable to Ca^{2+} and Ba^{2+} (H) and show low sensitivity to Ni^{2+} (I). (J) Bar graphs show the percentage change in control of T-type currents of three subunits for DTT modulation, permeability to Ca^{2+} versus Ba^{2+}, and Ni^{2+} inhibition.

The α1H subunit showed significantly higher sensitivity to Ni^{2+} inhibition than the other two subunits ($p < 0.05$). Error bars indicate the SD.

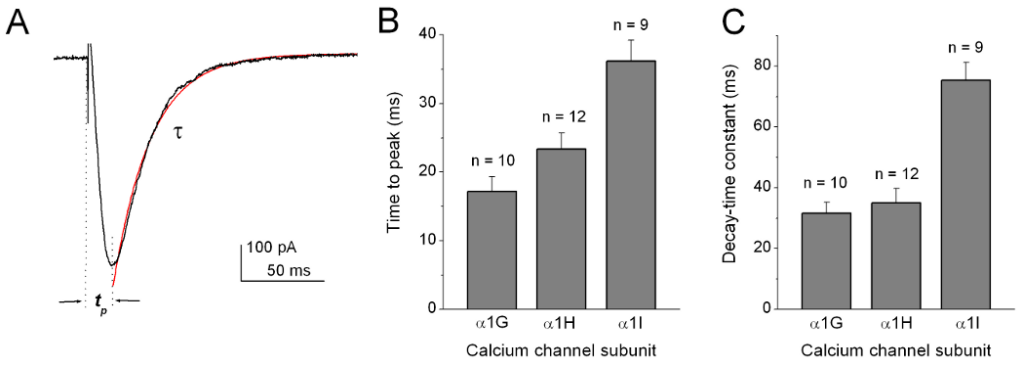

Figure 6. Summary of the kinetic properties of T-type Ca^{2+} currents from HEK-293 cells transiently expressing α1G, α1H, or α1I calcium channel subunits

(A) Typical recording of T-type currents and measurements of time-to-peak (t_p) values and the inactivation time constant (τ). Currents were evoked by a voltage pulse to -40 mV from a holding potential of -80 mV. (B) Average time-to-peak values and inactivation time constants of the T-type subunit currents.

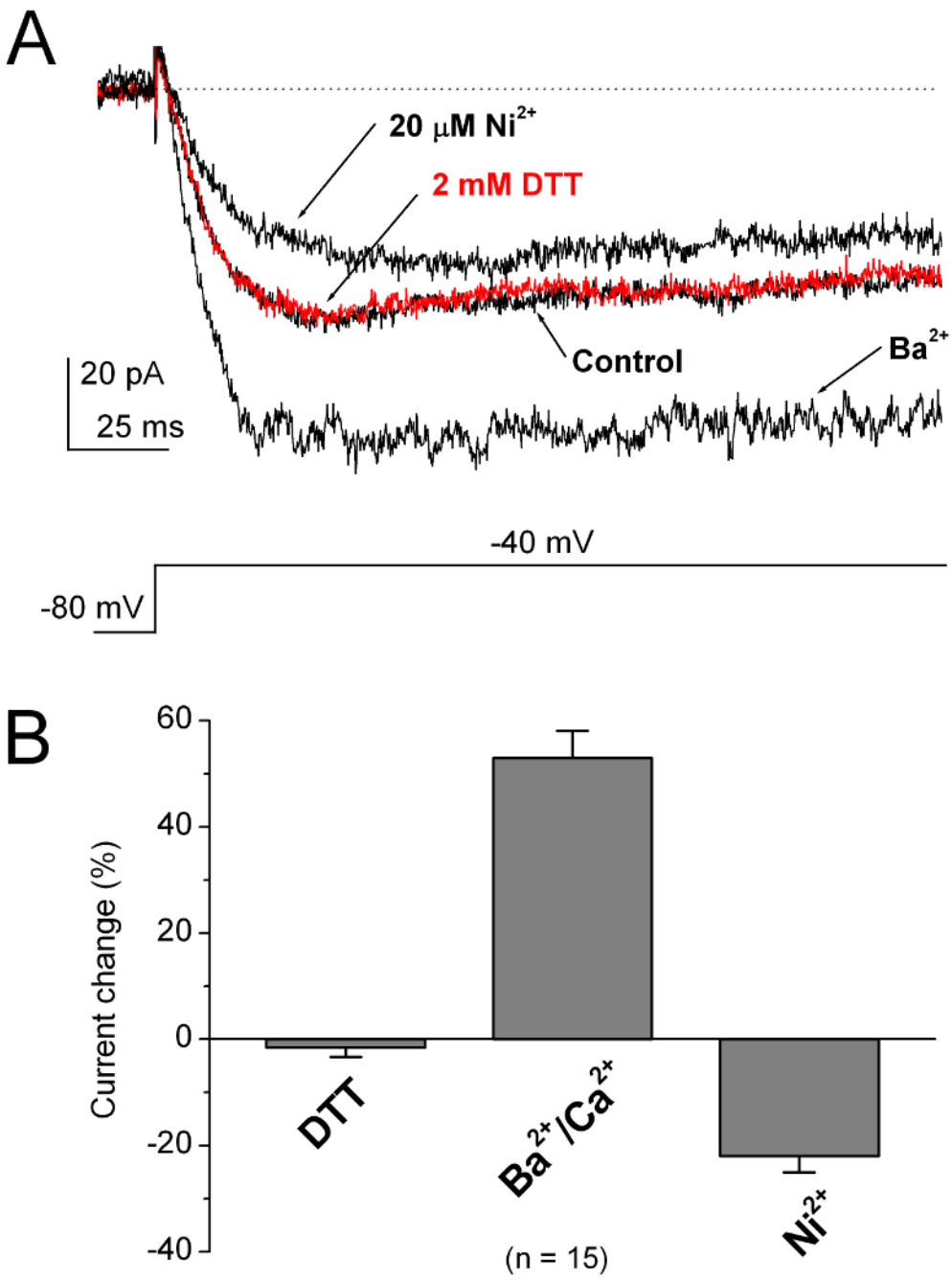

Figure 7. The properties of T-type Ca^{2+} currents in rod bipolar cells

(A) The T-type Ca^{2+} currents in rod bipolar cells were not modulated by 2 mM DTT. The currents showed more permeability to Ba^{2+} than to Ca^{2+}. These T-type currents were only slightly inhibited by 20 μM Ni^{2+}. (B) Bar graphs show the percentage change to control of T-type currents in rod bipolar cells on DTT modulation, permeability to Ca^{2+} versus Ba^{2+}, and Ni^{2+} inhibition. Error bars indicate the SD.

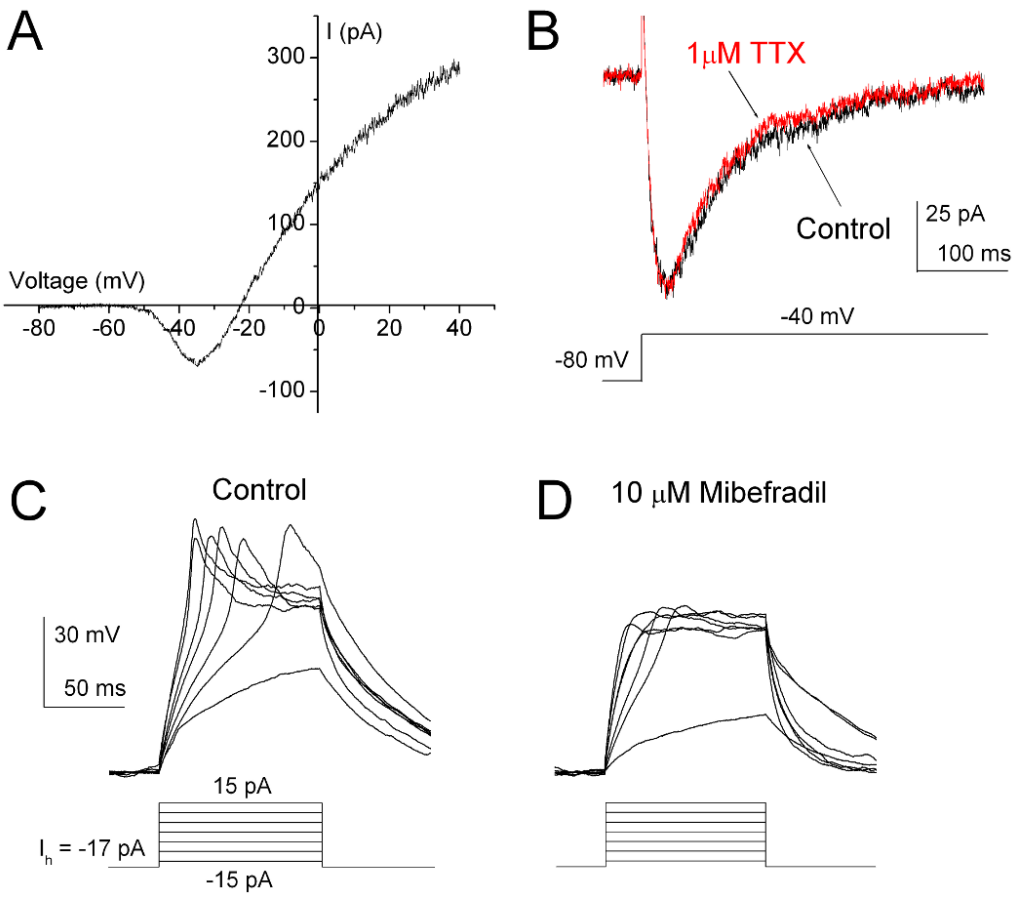

Figure 8. Low threshold spikes mediated by T-type Ca^{2+} currents

Recordings were made in an extracellular solution containing 2.5 mM Ca^{2+} without blockade of potassium channels. (A) The large voltage-gated K^+ currents did not mask the T-type currents but they did mask L-type currents in response to ramp stimulation voltage ranging from -80 mV to 40 mV (H_{hold} = -80 mV). (B) The step pulse to -40 mV evoked typical T-type currents (V_{hold} = -80 mV). The current was not affected by the application of 1 μM TTX. (C) The regenerative potentials were evoked in the current clamp mode. D, The regenerative potentials were blocked by 10 μM mibefradil.

Table 1

The summary and comparison of the T-type Ca^{2+} current properties between the three subgroups of T-rich cone bipolar cells (CBCs) and the three T-type Ca^{2+} channel subunits

The data for the DTT modulation are presented as the percentage of increase (+) or decrease (-) compared to control after the application of 2 mM DTT. The data for Ba^{2+}/Ca^{2+} permeability are presented as the percentage of the Ba^{2+} current normalized to the Ca^{2+} current when 10 mM extracellular Ca^{2+} was replaced by 10 mM Ba^{2+}. The data for Ba^{2+}/Ca^{2+} permeability are presented as the percentage of the Ba^{2+} current normalized to the Ca^{2+} current when 10 mM extracellular Ca^{2+} was replaced by 10 mM Ba^{2+}. The data for the Ni^{2+} sensitivity are presented as the percentage of the blockade after the application of 20 μM Ni^{2+}. All data are presented as mean ± SD from the indicated number of cells.

	CBC Subgroup 1 (n = 44)	**α1G (n = 10)**	**CBC Subgroup 2 (n = 29)**	**α 1H (n = 12)**	**CBC Subgroup 3 (n = 20)**	**α1I (n = 9)**
DTT modulation	-4.2 ±1.9	2.6 ± 2.7	32.2 ± 8.2	22 ± 5.2	-3.4 ± 1.7	4.0 ± 1.7
Ba^{2+}/Ca^{2+} permeability	75.5 ± 6.7	82 ± 4.7	145 ± 11	146 ± 11	99 ± 0.9	99 ± 0.5
Ni^{2+} sensitivity	-25.6 ± 6.0	-25.0 ± 6.0	-64 ± 11	-65 ± 15	-22 ± 8.0	-12 ± 8.0
Time to peak (ms)	19.5 ± 2.1	17.2 ± 2.2	24.7 ± 3.3	23.3 ± 2.4	34.8 ± 3.7	36.1 ± 3.1
Decay time (ms)	55.6 ± 3.8	31.6 ± 3.6	67.2 ± 6.2	35 ± 4.8	93.5 ± 5.8	75.4 ± 5.9